Proceedings of the 2006 IEEE International Conference on Robotics and Automation
Orlando, Florida - May 2006

Computing 3-Legged Equilibrium Stances in Three-Dimensional Gravitational Environments

Yizhar Or
Dept. of ME, Technion, Israel
izi@tx.technion.ac.il

Elon Rimon
Dept. of ME, Technion, Israel
rimon@tx.technion.ac.il

***Abstract*— Quasistatic multi-legged locomotion consists of a sequence of equilibrium postures where the mechanism supports itself against gravity while moving free limbs to new positions. A posture maintains equilibrium if the contacts can passively support the mechanism against gravity. This paper is concerned with identifying and computing equilibrium postures for mechanisms supported by frictional contacts in a three-dimensional gravitational field. The complex kinematic structure of the mechanism is lumped into a single rigid body $\mathcal{B}$ having the same contacts with the environment and a variable center of mass. The identification of equilibrium postures associated with a given set of contacts is reduced to the identification of center-of-mass locations of $\mathcal{B}$ that maintain equilibrium stances while all nonlinear frictional constraints are satisfied. Focusing on 3-contact stances, this paper provides an exact formulation for the boundary of the center-of-mass feasible region $\mathcal{R}$ as a solution of implicit polynomials. The paper also provides a conservative polyhedral approximation of $\mathcal{R}$ by using techniques for projection of convex polytopes. The exact and approximate computations of $\mathcal{R}$ are demonstrated with graphical examples.**

I. Introduction

Multi-legged robots that perform quasistatic locomotion are becoming progressively more sophisticated. Quasistatic multi-legged locomotion can be characterized as a sequence of postures where the mechanism supports itself against gravity while moving free limbs to new foothold positions. Autonomous planning of these motions requires tools for selecting postures that can stably support the mechanism against gravity while allowing motion of its free limbs to new positions.

This paper focuses on identifying and computing the feasible equilibrium postures of multi-legged mechanisms supported by 3 frictional contacts in a three-dimensional gravitational field. As a first step, the complex kinematic structure of the mechanism is lumped into a single rigid body $\mathcal{B}$ having the same contacts with the environment and a variable center of mass. The identification of the feasible equilibrium postures associated with a given set of contacts is reduced to the identification of center-of-mass locations that generate feasible equilibrium stances of $\mathcal{B}$, while satisfying friction constraints at the contacts. Stance stability received considerable attention in the literature discussing multi-legged locomotion. Notable early papers on multi-legged machines are [10], [15]. More recent papers that discuss stance stability appear in the literature on humanoid robots, e.g. [4], [8], [14]. When considering stance stability of legged robots, a leading concept is the *support polygon principle* [10], which states that the center-of mass must lie above the polygon spanned by the contacts. This principle was further extended for dynamic motion synthesis of humanoid robots with the concept of *zero moment point* (ZMP) [15]. However, these notions apply only for *flat terrains*, where contact normals are purely vertical. To our knowledge, no previous work on legged locomotion on 3D considered frictional supports on non-flat terrain. In the grasping literature, discussing frictional grasps in 3D, some works use polyhedral approximation of the quadratic friction cones [7],[13]. This approach enables formulation of equilibrium and grasp optimization as linear programs. Han et. al. [3] formulated the exact frictional constraints as a linear matrix inequality (LMI) problem, for testing force-closure and optimizing actuator torques. Using a different approach, Bicchi [2] formulated the force-closure test as a nonlinear differential equation. However, most of these works assume full actuation of the contact forces, while multi-legged mechanisms are supported by *passive* contacts that can only react to applied forces. Furthermore, multi-legged mechanisms have a variable shape due to internal joints, which is modelled in this work as a variable center of mass.

This paper is a continuation of two prior works. The work of Or and Rimon [11] which characterizes robust equilibrium postures in 2D, and the work of Mason et. al. [9] which characterizes equilibrium postures for frictionless contacts in 3D. This paper generalizes these works to three-dimensional environments with friction at the contacts. The main contribution of the paper are two methods for computing the center-of-mass feasible region $\mathcal{R}$ for 3-contact stances. The first method uses a geometric parametrization of the nine-dimensional space of contact forces to obtain the exact boundary of $\mathcal{R}$ as a solution of implicit polynomials. The second method

0-7803-9505-0/06/$20.00 ©2006 IEEE

formulates $\mathcal{R}$ as a projection of a five-dimensional set onto a two-dimensional plane, which leads to a conservative polyhedral approximation of $\mathcal{R}$.

The structure of the paper is as follows. In the next section we formulate the equilibrium condition, define the feasible center-of-mass region $\mathcal{R}$, and show some of its fundamental properties. In section III we focus on 3-contact stances, and define a geometric parametrization of the indeterminate contact forces. In section IV we use this parametrization to formulate the exact boundary of $\mathcal{R}$ in terms of high-order polynomials. In section V we show that computing $\mathcal{R}$ for 3 contacts can be formulated as a projection of a five-dimensional set onto a two-dimensional plane. Using a polyhedral approximation of the quadratic friction cones, we apply an efficient algorithm shown in [13] for projection of high-dimensional convex polytopes to derive a polyhedral approximation of $\mathcal{R}$. In the closing section we discuss limitations of our work and present relevant open problems. Due to lack of space, the proofs are relegated to Ref. [12].

II. Definition of Equilibrium Stances in 3D

In this section we define basic terminology, formulate the equilibrium conditions, and prove some basic properties of equilibrium stances in 3D. Let a solid object $\mathcal{B}$ be supported by k frictional contacts under gravity. Let x_i be the position of the i^{th} contact, and let f_i be the i^{th} contact reaction force. The static equilibrium condition is given by

$$\sum_{i=1}^{k} \begin{pmatrix} I \\ [x_i\times] \end{pmatrix} f_i = - \begin{pmatrix} I \\ [\boldsymbol{x}\times] \end{pmatrix} f_g \qquad (1)$$

where $\boldsymbol{x}$ is the position of $\mathcal{B}$'s center-of-mass, f_g is the gravitational force acting at $\boldsymbol{x}$, I is the 3×3 identity matrix, and $[a\times]$ is the 3×3 cross-matrix satisfying $[a\times]v = a\times v$ for all $v\in I\!R^3$. Note that for $k\geq 3$ contacts the static solution for $f_1\dots f_k$ is generically indeterminate of degree $3k-6$. Assuming Coulomb's friction model, the contact forces must additionally lie in their respective friction cones

$$\begin{aligned} \mathcal{C}_i = \{ & f_i : f_i\cdot n_i \geq 0 \\ & \text{and } (f_i\cdot s_i)^2 + (f_i\cdot t_i)^2 \leq (\mu f_i\cdot n_i)^2\}, \end{aligned} \qquad (2)$$

where μ is the coefficient of friction, n_i is the outward unit normal at x_i, and s_i, t_i are unit tangents at x_i such that (s_i, t_i, n_i) is a right-handed frame. The friction constraints can also be written as the following linear and quadratic inequalities;

$$\begin{aligned} &\mathcal{C}_i = \{f_i : f_i\cdot n_i \geq 0 \text{ and } f_i^T B_i f_i \leq 0\}, \text{ where} \\ &B_i = [s_i \;\; t_i \;\; n_i]\cdot \mathsf{diag}(1,1,-\mu^2)\cdot [s_i \;\; t_i \;\; n_i]^T. \end{aligned} \qquad (3)$$

In this work, we assume that all contacts are *upward pointing* as follows. Let $\boldsymbol{e} = (0\;\; 0\;\; 1)$ denotes the upward vertical direction, then all forces f_i in $\mathcal{C}_i$ must satisfy $f_i\cdot\boldsymbol{e}\geq 0$. This is a reasonable assumption in the context of legged locomotion, since relevant supports are generally located under the robot's footpads. A stance of $\mathcal{B}$ is defined by the contact points $x_1\dots x_k$ and the center-of-mass position $\boldsymbol{x}$. For a given set of contacts, the *feasible equilibrium region*, denoted $\mathcal{R}$, is all center-of-mass locations for which there exist contact reaction forces $f_i\in\mathcal{C}_i$ that satisfy the equilibrium equation (1). The goal of this paper is to compute the feasible region $\mathcal{R}$ for any given set of contacts. First we present three fundamental properties of $\mathcal{R}$, summarized in the following lemma.

Lemma II.1 ([12]). *Given a solid body $\mathcal{B}$ supported by k frictional contacts under gravity, the feasible equilibrium region $\mathcal{R}$, if nonempty, is an* **infinite vertical prism**. *The prism is connected and its cross-section is convex. Furthermore, the dimension of $\mathcal{R}$ for k contacts is generically* $\min\{3,k\}$.

The problem of computing $\mathcal{R}$ is thus reduced to computing its horizontal cross-section, denoted $\widetilde{\mathcal{R}}$, in $I\!R^2$. Since $k=3$ is the smallest number of contacts for which $\mathcal{R}$ is fully three-dimensional, this paper focuses on the computation of $\widetilde{\mathcal{R}}$ for 3-contact stances.

III. Parametrizing 3-Contact Reaction Forces

In this section we focus on 3-contact stances and present a geometric parametrization for the reaction forces satisfying the equilibrium equation (1) and the frictional constraints (3). The resulting parametrization would be in terms of the parameters $\boldsymbol{r}\in I\!R^2$ and $\boldsymbol{\zeta}\in I\!R^3$. This parametrization is used below for describing the feasible region $\mathcal{R}$. First, let us decompose each contact force into its horizontal and vertical projections,

$$\tilde{f}_i = E^T f_i,\;\; f_i^z = \boldsymbol{e}\cdot f_i, \text{ where } E = \begin{pmatrix} 1 & 0 \\ 0 & 1 \\ 0 & 0 \end{pmatrix}.$$

Similarly, let $\tilde{x}_i = E^T x_i$ and $x_i^z = \boldsymbol{e}\cdot x_i$ be the horizontal and vertical components of the contact points x_i, and let $\tilde{\boldsymbol{x}} = E^T\boldsymbol{x}$ be the horizontal component of the center-of-mass position $\boldsymbol{x}$. Then the equilibrium equation (1) can be divided into three equation sets [9]:

$$\begin{aligned} &a.\quad \textstyle\sum_{i=1}^3 \tilde{f}_i = 0_{2\times 1} \\ &\qquad \textstyle\sum_{i=1}^3 \tilde{x}_i^T J\tilde{f}_i = 0 \\ &b.\quad \textstyle\sum_{i=1}^3 f_i^z = 1 \\ &c.\quad \textstyle\sum_{i=1}^3 x_i^z J\tilde{f}_i + f_i^z J^T\tilde{x}_i = J^T\tilde{\boldsymbol{x}}, \end{aligned} \qquad (4)$$

where $J = \left[\begin{smallmatrix} 0 & -1 \\ 1 & 0 \end{smallmatrix}\right]$. Note that the force units are scaled such that $\|f_g\| = 1$. We will use (4a)-(4b) to obtain a parametrization of the contact forces, which will then imply a parametrization for $\tilde{\boldsymbol{x}}$ via (4c). The three scalar

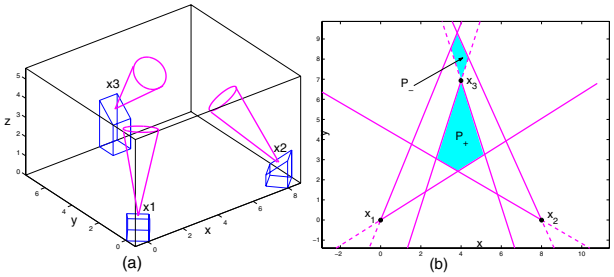

Fig. 1. (a) A 3-contact arrangement with $\mu = 0.2$, (b) horizontal projection of the contacts and friction cones, and the resulting region P (shaded).

equations in (4a) are force-and-torque balance of the 3 contact forces in a horizontal plane. These equations are independent of $\boldsymbol{x}$ and contain six scalar unknowns $\tilde{f}_1, \tilde{f}_2, \tilde{f}_3$. Hence they are indeterminate of degree 3. Let $\tilde{\mathcal{C}}_i$ be the horizontal projection of the friction cone $\mathcal{C}_i$. In order to satisfy the friction constraints $\tilde{f}_i$ must lie in $\tilde{\mathcal{C}}_i$. Since the horizontal forces $\tilde{f}_i$ generate zero net torque about a vertical axis, they must intersect at a common point in the horizontal plane. Let $\boldsymbol{r} \in I\!R^2$ denote this point. Since (4a) is homogenous in $\tilde{f}_i$, any particular choice of $\boldsymbol{r}$ determines $\tilde{f}_i$ up to a scaling factor $\sigma \in I\!R$. Therefore the pair $(\boldsymbol{r}, \sigma)$ fully parametrizes the $\tilde{f}_i$'s. Moreover, the frictional constraints imply that $\boldsymbol{r}$ must lie within a polygonal region in $I\!R^2$. These results are summarized in the following lemma.

Lemma III.1 ([12]). *Let $\boldsymbol{r}$ be a point in $I\!R^2$, and let $\sigma \in I\!R$ be a scaling factor. Then the horizontal contact forces solving eq. (4a) are parametrized by $(\boldsymbol{r}, \sigma)$ as $\tilde{f}_i = \sigma\lambda_i(\boldsymbol{r})(\boldsymbol{r} - \tilde{x}_i)$, where*

$$\lambda_i(\boldsymbol{r}) = (\boldsymbol{r} - \tilde{x}_{i+1}) \cdot J(\tilde{x}_{i+2} - \tilde{x}_{i+1}), \text{ for } i = 1,2,3 \quad (5)$$

and index addition is taken modulo 3.
Furthermore, for any nontrivial solution satisfying $\tilde{f}_i \in \tilde{\mathcal{C}}_i$, $\boldsymbol{r}$ must lie within the polygonal region $P = P_+ \cup P_-$, defined by:

$$\begin{aligned} P_+ &= \{\boldsymbol{r} \in I\!R^2 : \ \lambda_i(\boldsymbol{r})(\boldsymbol{r} - \tilde{x}_i) \in \tilde{\mathcal{C}}_i, \ i = 1,2,3\}, \\ P_- &= \{\boldsymbol{r} \in I\!R^2 : \ -\lambda_i(\boldsymbol{r})(\boldsymbol{r} - \tilde{x}_i) \in \tilde{\mathcal{C}}_i, \ i = 1,2,3\}. \end{aligned} \quad (6)$$

Example: Fig. 1(a) shows a 3-contact arrangement, together with the friction cones $\mathcal{C}_i$ for $\mu = 0.2$. Fig. 1(b) shows the projected contacts $\tilde{x}_i$ and friction cones $\tilde{\mathcal{C}}_i$ in a horizontal plane. The shaded region is $P = P_+ \cup P_-$, where $P_+ = \tilde{\mathcal{C}}_1 \cap \tilde{\mathcal{C}}_2 \cap \tilde{\mathcal{C}}_3$, and P_- is the intersection of $\tilde{\mathcal{C}}_1$ and $\tilde{\mathcal{C}}_2$ with the negative reflection of $\tilde{\mathcal{C}}_3$ about its base point $\tilde{x}_3$.

Next we extend the $(\boldsymbol{r}, \sigma)$ parametrization to a parametrization of the full contact forces by the pair $(\boldsymbol{r}, \boldsymbol{\zeta}) \in I\!R^2 \times I\!R^3$, where the intermediate parameter σ is eliminated. Recall that $\boldsymbol{r} \in I\!R^2$ is the intersection point of the $\tilde{f}_i$'s. Let l_r be the vertical line in $I\!R^3$ whose horizontal projection is $\boldsymbol{r}$. A natural choice for parametrizing the vertical component of f_i is ζ_i—the vertical distance between the contact x_i and the point where the line of f_i intersects the vertical line l_r. Let $\boldsymbol{\zeta} = (\zeta_1, \zeta_2, \zeta_3)$, and let Q be permissible region of $(\boldsymbol{r}, \boldsymbol{\zeta})$ implied by the frictional constraints (3). (See [12] for graphical illustration of ζ_i and of Q.) The following lemma summarizes the parametrization of the contact forces f_i by $(\boldsymbol{r}, \boldsymbol{\zeta})$, and formulates the permissible region Q.

Lemma III.2 ([12]). *The full contact forces solving equations (4a) and (4b) are parametrized by $(\boldsymbol{r}, \boldsymbol{\zeta}) \in I\!R^2 \times I\!R^3$ as follows:*

$$\begin{aligned} &f_i = \sigma(\boldsymbol{r}, \boldsymbol{\zeta})\lambda_i(\boldsymbol{r})(E(\boldsymbol{r} - \tilde{x}_i) + \zeta_i \boldsymbol{e}) \text{ for } i = 1,2,3, \\ &\text{where } \sigma(\boldsymbol{r}, \boldsymbol{\zeta}) = 1/(\lambda_1(\boldsymbol{r})\zeta_1 + \lambda_2(\boldsymbol{r})\zeta_2 + \lambda_3(\boldsymbol{r})\zeta_3), \end{aligned} \quad (7)$$

and $\lambda_i(\boldsymbol{r})$ are defined in (5). Furthermore, in order to satisfy $f_i \in \mathcal{C}_i$, the parameters $(\boldsymbol{r}, \boldsymbol{\zeta})$ must lie within a region $Q = Q_1 \cap Q_2 \cap Q_3$ defined by:

$$\begin{aligned} &Q_i = \{(\boldsymbol{r}, \boldsymbol{\zeta}) \in I\!R^2 \times I\!R^3 : \boldsymbol{r} \in P, \ \sigma(\boldsymbol{r}, \boldsymbol{\zeta})\lambda_i(\boldsymbol{r})\zeta_i \geq 0, \text{ and} \\ &\sigma(\boldsymbol{r}, \boldsymbol{\zeta})\lambda_i(\boldsymbol{r})(E(\boldsymbol{r} - \tilde{x}_i) + \zeta_i \boldsymbol{e})^T B_i (E(\boldsymbol{r} - \tilde{x}_i) + \zeta_i \boldsymbol{e}) \leq 0\}. \end{aligned} \quad (8)$$

Finally, in the next section we pay special attention to the boundary of Q, denoted ∂Q. It can be verified that on ∂Q at least one contact force f_i lies on the boundary of its friction cone $\mathcal{C}_i$. In this case the corresponding ζ_i can be expressed in terms of $\boldsymbol{r}$ as follows. Using the quadratic friction constraint in (8), a nonzero ζ_i must satisfy $(E(\boldsymbol{r} - \tilde{x}_i) + \zeta_i \boldsymbol{e})^T B_i (E(\boldsymbol{r} - \tilde{x}_i) + \zeta_i \boldsymbol{e}) = 0$. The solution $\zeta_i^*(\boldsymbol{r})$ of this quadratic equation is given by

$$\begin{aligned} &\zeta_i^*(\boldsymbol{r}) = \tilde{b}_i^T(\boldsymbol{r} - \tilde{x}_i) \pm \sqrt{(\boldsymbol{r} - \tilde{x}_i)^T \tilde{B}_i (\boldsymbol{r} - \tilde{x}_i)}, \\ &\text{where } \tilde{b}_i = -\frac{1}{\boldsymbol{e}^T B_i \boldsymbol{e}} E^T B_i \boldsymbol{e} \text{ and} \\ &\tilde{B}_i = \frac{1}{(\boldsymbol{e}^T B_i \boldsymbol{e})^2} E^T B_i [(\boldsymbol{e}\boldsymbol{e}^T) - (\boldsymbol{e}^T B_i \boldsymbol{e}) I_{3\times 3}] B_i E. \end{aligned} \quad (9)$$

IV. Computing Stances by Parametrization

We now use the contact force parameterization to compute the feasible region $\mathcal{R}$. First, we define a map $\Phi : Q \to I\!R^2$ from $(\boldsymbol{r}, \boldsymbol{\zeta})$ to the feasible center-of-mass horizontal positions $\tilde{\boldsymbol{x}}$. Then we compute the exact boundary of $\widetilde{\mathcal{R}}$ as the image of critical points of Φ on Q. Finally, we demonstrate the exact computation with a graphical example.

A. Using the $(\boldsymbol{r}, \boldsymbol{\zeta})$ Parametrization to Compute $\mathcal{R}$

The three reaction forces are parametrized by $(\boldsymbol{r}, \boldsymbol{\zeta}) \in Q$, where $Q \subset I\!R^2 \times I\!R^3$ is defined in (8). Recall that the equilibrium condition were grouped into three sets in (4), such that only eq. (4c), which is torque balance about horizontal axes, depends on $\tilde{\boldsymbol{x}}$. Using the parametrization (7), eq. (4c) defines a map $\Phi : Q \to I\!R^2$ from $(\boldsymbol{r}, \boldsymbol{\zeta})$ to the horizontal center-of-mass positions $\tilde{\boldsymbol{x}}$ that generate an equilibrium stance:

$$\tilde{\boldsymbol{x}} = \Phi(\boldsymbol{r},\boldsymbol{\zeta}) = \sigma(\boldsymbol{r},\boldsymbol{\zeta}) \sum_{i=1}^{3} \lambda_i(\boldsymbol{r})[-x_i^z(\boldsymbol{r}-\tilde{x}_i)+\zeta_i\tilde{x}_i], \quad (10)$$

where $\lambda_i(\boldsymbol{r})$ are defined in (5) and $\sigma(\boldsymbol{r},\boldsymbol{\zeta})$ is defined in (7). The horizontal cross-section of $\mathcal{R}$ is precisely the image of Q under Φ. This image cannot be simply computed, since Φ is highly nonlinear in $(\boldsymbol{r},\boldsymbol{\zeta})$ and Q has a complex structure. However, the boundary of $\mathcal{R}$ is the image of critical points of Φ on Q, which can be computed in closed form as follows.

B. Computing Critical Curves of Φ

The boundary curves of the image of Q under Φ are image of critical curves of Φ in Q, on which the Jacobian matrix $D\Phi$ is not full rank. The critical curves can be classified into four classes from type-1 to type-3. Type-n curve consists of points $(\boldsymbol{r},\boldsymbol{\zeta})$ parametrizing contact forces such that n forces lie on the boundary of their friction cones. The following proposition formulates all types of critical curves as solutions of implicit equations.

Proposition IV.1 ([11]). *Let $\Phi : Q \to I\!R^2$ be the map of $(\boldsymbol{r},\boldsymbol{\zeta})$ to $\tilde{x}$. The three types of critical curves of Φ are:*

Type 1 critical curves: *Type 1 Critical curve have $\boldsymbol{r}$-component that lies on a straight line segment passing through a pair of projected contact points $\tilde{x}_i$ and $\tilde{x}_j$, as long as this segment intersects the polygonal region P.*

Type 2 critical points: *Type 2 critical curves are straight lines in $(\boldsymbol{r},\boldsymbol{\zeta})$ space, having $\boldsymbol{r}$ fixed at $\boldsymbol{r}^*, \zeta_2$ and ζ_3 fixed at $\zeta_2^*(\boldsymbol{r}^*)$ and $\zeta_3^*(\boldsymbol{r}^*)$ as defined in (9), while ζ_1 varies freely. (The contacts' indices can be arbitrarily permuted). The fixed value of $\boldsymbol{r}$ is the solution of the two implicit equations $\det[M_2(\boldsymbol{r})] = 0$, and $\det[N_2(\boldsymbol{r})] = 0$, where $M_2(\boldsymbol{r})$ and $N_2(\boldsymbol{r})$ are obtained by composition of the following functions:*

$$\begin{aligned}
&N_2(\boldsymbol{r}) = \left[M_2(\boldsymbol{r}) \begin{pmatrix} 0 \\ 1 \end{pmatrix} \quad \tilde{x}_1 + \boldsymbol{u}(\boldsymbol{r}) \right] \\
&M_2(\boldsymbol{r}) = \big[\textstyle\sum_{j=2}^{3} \lambda_j(\boldsymbol{r})\zeta_j^*(\boldsymbol{r})\big] \big[\textstyle\sum_{i=1}^{3} x_i^z(\lambda_i(\boldsymbol{r})I \\
&+(\boldsymbol{r}-\tilde{x}_i)\lambda_i'(\boldsymbol{r})) - \textstyle\sum_{i=2}^{3}(\lambda_i(\boldsymbol{r})\zeta_i'(\boldsymbol{r})+\zeta_i^*(\boldsymbol{r})\lambda_i'(\boldsymbol{r}))\tilde{x}_i\big] \\
&\quad -\big[\textstyle\sum_{i=1}^{3} \lambda_i(\boldsymbol{r})x_i^z(\boldsymbol{r}-\tilde{x}_i) - \textstyle\sum_{i=2}^{3} \lambda_i(\boldsymbol{r})\zeta_i^*(\boldsymbol{r})\tilde{x}_i)\big] \\
&\quad \cdot\big[\textstyle\sum_{j=2}^{3} \lambda_j(\boldsymbol{r})\zeta_j'(\boldsymbol{r})+\zeta_j^*(\boldsymbol{r})\lambda_j'(\boldsymbol{r})\big], \text{ where} \\
&\boldsymbol{u}(\boldsymbol{r}) = \tfrac{1}{\lambda_2(\boldsymbol{r})\zeta_2^*(\boldsymbol{r})+\lambda_3(\boldsymbol{r})\zeta_3^*(\boldsymbol{r})} \{\textstyle\sum_{i=1}^{3}[x_i^z\lambda_i(\boldsymbol{r})(\boldsymbol{r}-\tilde{x}_i)] \\
&\quad -\lambda_2(\boldsymbol{r})\zeta_2^*(\boldsymbol{r})\tilde{x}_2 - \lambda_3(\boldsymbol{r})\zeta_3^*(\boldsymbol{r})\tilde{x}_3\} \\
&\lambda_i'(\boldsymbol{r}) = (\tilde{x}_{i+2} - \tilde{x}_{i+1})^T J^T \\
&\zeta_i'(\boldsymbol{r}) = \tilde{b}_i^T \pm \tfrac{1}{\sqrt{(\boldsymbol{r}-\tilde{x}_i)^T\tilde{B}_i(\boldsymbol{r}-\tilde{x}_i)}} (\boldsymbol{r}-\tilde{x}_i)^T\tilde{B}_i
\end{aligned} \quad (11)$$

$\lambda_i(\boldsymbol{r})$ are defined in (5), $\zeta_i^*(\boldsymbol{r}), \tilde{b}_i, \tilde{B}_i$ are defined in (9), and I is the 2×2 identity matrix.

Type 3 critical points: *There are two cases of type 3 critical curves:*

Type 3A curves have $\boldsymbol{r}$ component lying on the boundary ∂P, while $\zeta_i = \zeta_i^*(\boldsymbol{r})$ as defined in (9). These curves can be explicitly formulated as a function of a single parameter $s \in [0,1]$ as follows

$$\boldsymbol{r}(s) = s\boldsymbol{v}' + (1-s)\boldsymbol{v}'' \ , \ \ \zeta_i(s) = \zeta_i^*(\boldsymbol{r}(s)), \quad (12)$$

where $\boldsymbol{v}', \boldsymbol{v}''$ are two adjacent vertices of the polygonal region P.

Type 3B curves have $\boldsymbol{r}$ component lying within the interior of P, while $\zeta_i = \zeta_i^*(\boldsymbol{r})$ as defined in (9). The $\boldsymbol{r}$ component lies on the curve which is the solution of the implicit equation $\det[M_3(\boldsymbol{r})] = 0$, where $M_3(\boldsymbol{r})$ is obtained by composition of the following functions:

$$\begin{aligned}
&M_3(\boldsymbol{r}) = \textstyle\sum_{i=1}^{3}\{[(-x_i^z(\boldsymbol{r}-\tilde{x}_i)+\zeta_i^*(\boldsymbol{r}))\tilde{x}_i\lambda_i'(\boldsymbol{r}) \\
&\quad +\lambda_i(\boldsymbol{r})(-x_i^z I + \tilde{x}_i\zeta_i'(\boldsymbol{r}))][\textstyle\sum_{j=1}^{3} \lambda_j(\boldsymbol{r})\zeta_j^*(\boldsymbol{r})] \\
&\quad +\lambda_i(\boldsymbol{r})(x_i^z(\boldsymbol{r}-\tilde{x}_i)-\zeta_i^*(\boldsymbol{r})\tilde{x}_i)[\textstyle\sum_{j=1}^{3} \lambda_j(\boldsymbol{r})\zeta_j'(\boldsymbol{r}) \\
&+\zeta_j^*(\boldsymbol{r})\lambda_j'(\boldsymbol{r})]\},
\end{aligned}$$

where $\lambda_i'(\boldsymbol{r})$ and $\zeta_i'(\boldsymbol{r})$ are defined in (11), $\lambda_i(\boldsymbol{r})$ are defined in (5), $\zeta_i^*(\boldsymbol{r})$ are defined in (9), and I is the 2×2 identity matrix. (13)

Proof outline: First, recall that criticality conditions also hold under change of coordinates. Second, notice that type-j critical curves lie in a $(5\text{–}j)$-dimensional submanifold of Q. For each type of critical curve, we express the restriction $\bar{\Phi}$ of Φ to the corresponding sumbmanifold of Q with a reduced set of new coordinates. Then we explicitly compute the Jacobian $D\bar{\Phi}$, and formulate the conditions for its rank deficiency. □

We have formulated all the critical curves in $(\boldsymbol{r},\boldsymbol{\zeta})$-space, whose Φ-image are candidate boundary curves of $\widetilde{\mathcal{R}}$. In order to complete the computation, one needs to find these curves, and compute their associated image under Φ. This results in a planar arrangement of candidate boundary curves in $\tilde{x}$-plane. Finally, the actual boundary consists of the "outmost" curves, and can be found by taking the convex hull of all curves. (See [1],[6] for details about computing convex hull of parametric curves.) The following corollary summarizes these concluding steps.

Corollary IV.2. *Given a solid body $\mathcal{B}$ supported by 3 frictional contacts in a 3D gravitational field, the center-of-mass feasible equilibrium region is a vertical prism, whose horizontal cross-section can be computed by the following steps:*

1. *If any of the line segments $\tilde{x}_i - \tilde{x}_j$ intersect the polygonal region P, compute the corresponding line segment in $\tilde{\boldsymbol{x}}$-plane, associated with two active contacts exerting forces only in the vertical plane containing $\tilde{x}_i$ and $\tilde{x}_j$, using the planar analysis detailed in [11].*

2. *Compute type 2 critical curves, which are solutions of the implicit equations $\det[M_2(\boldsymbol{r})] = 0, \det[N_2(\boldsymbol{r})] = 0$ defined in (11). The Φ-image of these curves, obtained by*

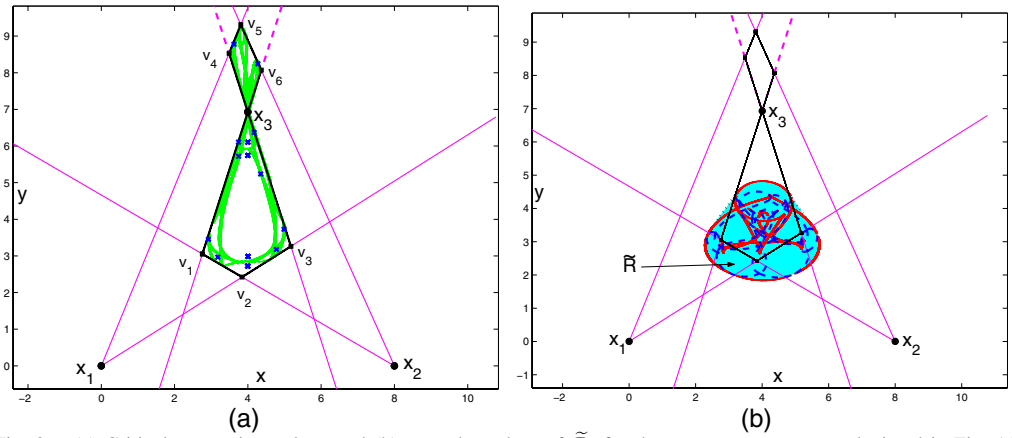

Fig. 2. (a) Critical curves in $\boldsymbol{r}$-plane and (b) exact boundary of $\widetilde{\mathcal{R}}$, for the contact arrangement depicted in Fig. 1(a)

substitution into (10), contributes additional candidate boundary curves.

3. *Compute type 3A critical curves as formulated in (11). The* Φ*-image of these curves, obtained by substitution into (10), contributes additional candidate boundary curves.*

4. *Compute type 3B critical curves, which are solutions of the implicit equation* $\det[M_3(\boldsymbol{r})] = 0$ *defined in (13). The* Φ*-image of these curves, obtained by substitution into (10), contributes additional candidate boundary curves.*

5. *Finally, the convex hull enclosing all the obtained candidate curves is the cross-section* $\widetilde{\mathcal{R}}$*.*

Example: Fig. 2(a) shows the $\boldsymbol{r}$-component of all critical curves for the 3-contact arrangement depicted in Fig. 1(a). Recall that the $\boldsymbol{r}$-component of type 3A curves is simply the boundary of the polygonal region P. The $\boldsymbol{r}$-component of type 3B curves are the solid lines within P. The $\boldsymbol{r}$-component of type 2 critical curves are isolated points, marked by $'\times'$. Fig. 2(b) shows in $\tilde{\boldsymbol{x}}$-plane the Φ-image of type 3A critical curves (dashed), of type 3B critical curves (solid), and of type 2 critical curves (dotted line segments, only those contributing to the actual boundary are drawn), for same 3-contact arrangement. Note that all types of candidate boundary curves are required to enclose a convex region, which is the resulting exact cross-section $\widetilde{\mathcal{R}}$ (shaded region).

V. Computing Stances by Projection

In this section we show that for 3-contacts arrangements $\widetilde{\mathcal{R}}$ can be conservatively approximated as a projection of a five-dimensional polytope onto a two-dimensional plane. First we define the *equilibrium space* as a five-dimensional space combining center-of-mass locations and contact forces satisfying the equilibrium condition. Then we approximate the quadratic friction cones by inscribed polyhedra. The linearized frictional constraints define a feasible region in the equilibrium space, whose projection onto $\tilde{\boldsymbol{x}}$-plane gives the polygonal approximation of the cross-section $\widetilde{\mathcal{R}}$. The approximate region is demonstrated graphically, and compared with the exact results obtained by the parametrization approach.

Consider a solid body $\mathcal{B}$ supported by 3 frictional contacts in a three-dimensional gravitational field. Define $\boldsymbol{f} = (f_1, f_2, f_3) \in I\!R^9$ as the combined forces vector. Scaling force units such that $\|f_g\| = 1$, the equilibrium condition (1) can be written in matrix form as

$$\begin{aligned} &G\boldsymbol{f} = T\tilde{x} + u_o, \\ &\text{where } G = \begin{pmatrix} I & I & I \\ [x_1\times] & [x_2\times] & [x_3\times] \end{pmatrix}, \\ &T = \begin{pmatrix} 0_{3\times 2} \\ EJ^T \end{pmatrix}, \quad u_o = \begin{pmatrix} \boldsymbol{e} \\ \vec{0} \end{pmatrix}, \end{aligned} \tag{14}$$

and $\tilde{x}$ is the horizontal projection of the center-of-mass location. The static response is indeterminate of degree 3. Therefore, the static forces f_i can be expressed by $\boldsymbol{\eta} \in I\!R^3$ and $\tilde{\boldsymbol{x}} \in I\!R^2$, as

$$\boldsymbol{f} = M_\eta \boldsymbol{\eta} + M_x \tilde{\boldsymbol{x}} + \boldsymbol{\eta}_o, \tag{15}$$

where $M_\eta \in I\!R^{9\times 3}$ is a matrix whose columns span the nullspace of G, $M_x = G^\dagger T$ and $\boldsymbol{\eta}_o = G^\dagger u_o$, where $G^\dagger \in I\!R^{9\times 6}$ is a left pseudo-inverse of G. The pair $(\tilde{\boldsymbol{x}}, \boldsymbol{\eta})$ parametrizes all center-of-mass locations and contact forces satisfying the equilibrium condition (14). We now approximate the frictional constraints by linear constraints, and formulate the region in equilibrium space satisfying these constraints (See [12] for a discussion about using the exact frictional constraints). A friction cone in 3D can be conservatively approximated by an n-sided inscribed polyhedron, such that the quadratic constraint in (2) is replaced with n linear constraints. The approximate polyhedron $\mathcal{C}'_i$ is defined by

$$\begin{aligned} \mathcal{C}'_i = \{f_i : &(\sin\theta_{j+1} - \sin\theta_j)(f_i \cdot s_i) \\ &+ (\cos\theta_j - \cos\theta_{j+1})(f_i \cdot t_i) \le \beta(f_i \cdot n_i)\ ,\ j = 1 \dots n\}, \end{aligned} \tag{16}$$

where $\theta_j = \frac{2\pi j}{n}$, $\beta = \mu \sin\left(\frac{2\pi}{n}\right)$, μ is the coefficient of friction, and (s_i, t_i, n_i) is a right-handed orthonormal frame of two unit tangents and an outward unit normal at

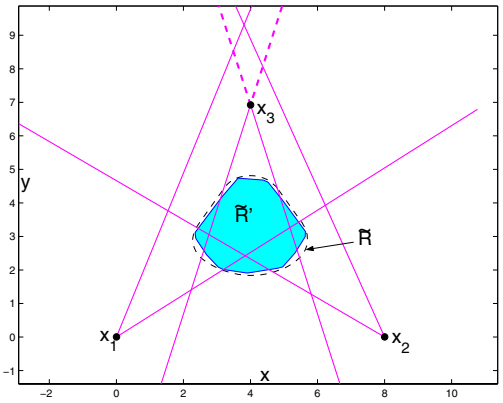

Fig. 3. Polygonal approximation $\widetilde{\mathcal{R}}'$ and the exact boundary of $\widetilde{\mathcal{R}}$ (dashed) for the contact arrangements depicted in Fig. 1(a).

x_i. The linear constraints can be written in matrix form as $A_i f_i \leq 0$, where

$$A_i = \begin{pmatrix} \sin\theta_2 - \sin\theta_1 & \cos\theta_1 - \cos\theta_2 & -\beta \\ \vdots & \vdots & \vdots \\ \sin\theta_1 - \sin\theta_n & \cos\theta_n - \cos\theta_1 & -\beta \end{pmatrix} \begin{pmatrix} s_i & t_i & n_i \end{pmatrix}^T.$$

Using the equilibrium space parametrization (15), the approximated feasible region in $(\tilde{\boldsymbol{x}}, \boldsymbol{\eta})$ space is the convex polytope defined by

$$\mathcal{S}' = \{(\tilde{\boldsymbol{x}}, \boldsymbol{\eta}) : \ \bar{A}_i(M_\eta \boldsymbol{\eta} + M_x \tilde{\boldsymbol{x}} + \boldsymbol{\eta}_o) \leq 0, \ \text{for } i = 1 \ldots 3\} \tag{17}$$

Where $\bar{A}_i$ is a proper augmentation of A_i in a block-diagonal matrix of dimensions $3n \times 9$. The projection of $\mathcal{S}'$ onto $\tilde{\boldsymbol{x}}$-plane is the polygonal approximation of $\widetilde{\mathcal{R}}$. Such a projection is a classical problem widely explored in computational geometry literature (e.g. [5]). In the following example, we implement an adapted version of the efficient contour-tracking algorithm proposed by Ponce et. al. [13] for projection of a high-dimensional convex polytope onto a lower dimensional space, in the context of grasp planning.

Example: Fig. 3 shows the conservative polygonal approximation $\widetilde{\mathcal{R}}'$ (shaded region) compared with the exact boundary of $\widetilde{\mathcal{R}}$ (dashed) for the 3-contact arrangements depicted in Fig. 1(a). The friction cones were approximated by six-sided polyhedra.

VI. Conclusion

We have shown that the center-of-mass feasible equilibrium region $\mathcal{R}$ for a k-contact stance is a vertical convex prism. For the 3-contact case, we defined a geometric parametrization of the indeterminate contact forces by five scalar parameters, and expressed the exact boundary as solutions of a high-degree polynomials. We also formulated the feasible region as the projection of a five-dimensional region onto a plane. Then we derived a polyhedral approximation of $\mathcal{R}$ which is based on the projection approach. The exact and approximate computations were demonstrated with graphical examples.

We now discuss two possible directions for future research. First, the 3-contacts critical curves were formulated as solutions of high-degree algebraic equations, and lack a simple geometric characterization. A geometric characterization of the criticality condition in these equations could provide insight that would simplify the exact computation of $\mathcal{R}$. It may also be helpful in generalizing the parametrization approach to higher number of contacts. Second, the feasible equilibrium region was computed while considering the single load of gravity. However, in practice one must consider stances which are *robust* with respect to a given neighborhood of disturbance wrenches surrounding the nominal gravitational wrench [11]. The characterization of *robust equilibrium stances* in three-dimensional environments is currently under investigation.

References

[1] C. L. Bajaj and M-S. Kim, "Convex Hulls of Objects Bounded by Algebraic Curves," *Algorithmica*, vol. 6, no. 4, pp. 533–553, 1991.

[2] A. Bicchi, "On the closure properties of robotic grasping," *The Int. J. of Robotics Research*, vol. 14, no. 4, pp. 319–334, 1995.

[3] L. Han, J. Trinkle, and Z. Li, "Grasp analysis as linear matrix inequality problems," *IEEE Trans. on Robotics and Automation*, vol. 16, no. 6, pp. 663–674, 2000.

[4] K. Hirai, M. Hirose, Y. Haikawa, and T. Takenaka, "The development of honda humanoid robot," in *IEEE Int. Conf. on Robotics and Automation*, 1998, pp. 1321–1326.

[5] T. Huynh, C. Lassez, and J.-L. Lassez, "Practical issues on the projection of polyhedral sets." *Ann. Math. Artif. Intell.*, vol. 6, no. 4, pp. 295–315, 1992.

[6] Yan-Bin Jia, "On the convex hulls of parametric plane curves ," http://www.cs.iastate.edu/ jia, Tech. Report, 2005.

[7] J. R. Kerr and B. Roth, "Analysis of multi-fingered hands," *The Int. J. of Robotics Research*, vol. 4, no. 4, 1986.

[8] J. Kuffner, K. Nishiwaki, S. Kagami, M. Inaba, and H. Inoue, "Motion planning for humanoid robots under obstacle and dynamic balance constraints," in *IEEE Int. Conf. on Robotics and Automation*, 2001, pp. 692–698.

[9] R. Mason, J. W. Burdick, and E. Rimon, "Stable poses of three-dimensional objects," in *IEEE Int. Conf. on Robotics and Automation*, pp. 391–398, 1997.

[10] R. McGhee and A. Frank, "On the stability properties of quadruped creeping gaits," *Mathematical Biosciences*, vol. 3, no. 3–4, pp. 331–351, 1968.

[11] Y. Or and E. Rimon, "Computation and graphic characterization of robust multiple-contact postures in gravitational environments," in *IEEE Int. Conf. on Robotics and Automation*, pp. 248–253, 2005.

[12] Y. Or and E. Rimon, "Computation of multiple-contact frictional equilibrium postures in three-dimensional gravitational environments," http://robots.technion.ac.il/publications, Tech. Report, 2005.

[13] J. Ponce, S. Sullivan, A. Sudsang, J.-D. Boissonnat, and J.-P. Merlet, "On computing four-finger equilibrium and force-closure grasps of polyhedral objects," *The Int. J. of Robotics Research*, vol. 16, no. 1, pp. 11–35, 1997.

[14] T. Sugihara and Y. Nakamura, "Whole-body cooperative COG control through ZMP manipulation for humanoid robots," in *2nd Int. Symp. on Adaptive Motion of Animals and Machines(AMAM2003)*, 2003.

[15] M. Vukobratovic, A. Frank, and D. Juricic, "On the stability of biped locomotion," in *IEEE Trans Biomed Eng*, vol. 17, no. 1, 1970, pp. 25–36.